Int. J. Electrochem. Sci., 11 **(2016)** 566 - 576

International Journal of
ELECTROCHEMICAL
SCIENCE
www.electrochemsci.org

Addition Effect of Fluoride Compounds for Zr Electrorefining in LiCl-KCl Molten Salts

Chang Hwa Lee[1,*], *Deok Yoon Kang*[1], *Min Ku Jeon*[1], *Kweon Ho Kang*[1], *Seung-Woo Paek*[1], *Do-Hee Ahn*[1] *and Kyoung-Tae Park*[2]

[1]Nuclear Fuel Cycle Process Process Development Division, Korea Atomic Energy Research Institute, 989-111 Daedeok-daero, Yuseong-gu, Daejeon 305-353, Republic of Korea
[2]Rare Metal R&BS Group, Korea Institute of Industrial Technology, Gaetbeol-ro 156, Yeonsu-gu, Incheon, 406-840, Republic of Korea
[*]E-mail: chwalee@kaeri.re.kr

Received: 16 September 2015 / *Accepted:* 31 October 2015 / *Published:* 1 December 2015

The effect of fluoride compounds on Zr electrorefining is investigated for Zirlo cladding tubes in LiCl-KCl based molten salts. Cyclic voltammetric curves exhibit a modification of electrochemical behaviors of Zr ions from a two-step reduction process in LiCl-KCl-0.07 M $ZrCl_4$ salts to one-step reduction by the addition of 0.84 M LiF. Morphological features of Zr deposits are found to also be changed from a powder type to a dendritic characteristic, thereby reducing the amount of incorporated salts and enhancing the crystallinity of electrorefined Zr. Quantitative measurement reveals that the Zr content in the deposit is increased by the addition of fluoride compounds, which is expected to enhance the recovery yield of Zr.

Keywords: Zirconium, Electrorefining, Zirlo, Fluoride, Molten Salt

1. INTRODUCTION

The pyrometallurgical process is known to be a highly proliferation-resistant technology for the treatment of used nuclear fuels (UNFs), which enables reducing the weight/volume of high-level waste through the electrochemical recovery of uranium (U) and transuranic (TRU) elements [1,2]. The pyroprocess developed at KAERI consists of a head-end process that produces feed materials through the disassembly, chopping, and decladding of fuel rods and a back-end process that recovers U and

Note: This paper was presented at 226th ECS meeting in Cancun. (C. H. Lee et al, ECS Transactions, 64 (2014) 609).

TRU from the feed materials through a series of electrochemical processes using electroreduction, electrorefining, and electrowining in molten salts [3].

In the pretreatment process, metal wastes including cladding hulls and hardware are expected to be produced by as much as around 2.5 tons and 1.0 tons per 10 tons of U, respectively. In particular, the cladding hull waste, which is composed of Zr alloys, would possibly be categorized as an intermediate level or a GTCC (greater than class C) level waste, because the cladding tube could include highly radioactive fission products generated during the reactor operation and a trace of UNF residue on the surface [4,5]. Therefore, the volume/weight reduction of metal wastes could be as important as the treatment of UNFs for the successful implementation of the pyroprocess.

Among the various technologies for the treatment of metal waste [6], compaction and melting processes that are commercially available can be used to reduce the volume of the wastes; however, the radioactivity level of the total waste cannot be changed. Therefore, alternative technologies that can separate the radioactive nuclides are necessary to effectively reduce the waste amount and lower the waste level. In this regard, chlorination and electrorefining can be utilized as alternative technologies because both the amount of total wastes and the waste level can be reduced by recovering Zr comprising about 98 wt% of Zr-alloy cladding tubes such as Zircaloy and Zirlo.

The electrorefining process is a technology that is able to electrochemically recover Zr on a cathode with a simultaneously occurring anodic dissolution of cladding hull wastes in high temperature molten salt electrolytes by applying a constant voltage or a constant current [7-10]. The electrorefining process is advantageous in recovering a high purity of Zr as a metallic form with a lower process cost and a higher conversion efficiency compared to the chlorination combined with the conventional Kroll process [11]. The electrochemical behaviors of Zr have been studied using potentiostatic/galvanostatic measurements in various molten salt systems [12-20]. For Zr deposition, LiCl-KCl eutectic salts have been widely used because of their lower operating temperatures and corrosiveness compared with fluoride-based salts. However, powder-type deposit characteristics of Zr electrorefined in most chloride-based molten salts cause a decrease in the recovery rate owing to a significant amount of salt incorporation in the deposit as well as a poor adhesion property [21]. In addition, a multi-step reduction process of Zr generally found in chloride-based salts makes a current control difficult and lowers the current efficiency [22]. On the other hand, all fluoride-based salts such as FLINAK (LiF-NaF-KF) are known to enable the formation of a dendritic Zr deposit, [15, 23, 24] which is possibly led by a single-step reduction of Zr^{4+} stabilized with F^- ions. However, the realization of the process using fluoride salt requires several challenges for the hull waste treatment because of their high melting points and strong corrosivities. In addition, the treatment and recycling process of the fluoride salt waste are required to be established for the application of all-fluoride salts.

In this regard, this paper investigates the electrochemical behavior of Zr in chloride-fluoride mixed salts by adding fluoride compounds as an initiator or a fluoride component in chloride-based salts. The effect of fluoride compounds on the morphological feature of Zr deposits will also be examined. This work will contribute to enhancing the recovery yield of Zr by reducing the incorporated salt.

2. EXPERIMENTAL

An anhydrous LiCl-KCl eutectic salt (99.99 wt% purity, Sigma-Aldrich) was used as a base electrolyte for the experiment. To examine the effect of fluoride ions, 0.07 M of ZrF_4 (99.9 wt% purity, Sigma-Aldrich) was added as a form of initiator for Zr electrorefining in LiCl-KCl salts. In addition, the concentration of fluoride ions was separately controlled by adding 0.84 M LiF (98 wt% purity, Wako) in LiCl-KCl containing 0.07 M $ZrCl_4$ (99.5 wt% purity, Sigma-Aldrich). All experiments were conducted in an Ar-purging glove box, in which the oxygen and moisture are controlled within 1 ppm. Cyclic voltammetric measurements were performed to investigate the electrochemical behavior of Zr in various molten salt systems using potentiostat/galvanostat (BioLogics SP-150) under quiescent conditions. Tungsten wires (1 mm dia.) shielded with alumina tubes were used as a working electrode with an exposed area of 0.950 cm^2. Zr rods (6 mm dia.) were used as an anode for electrochemical measurements. The reference electrode was made with an Ag wire placed in a mullite tube filled with LiCl-KCl-1 wt% AgCl salts. The operating temperature was fixed at 600 ^oC for LiCl-KCl-$ZrCl_4$, LiCl-KCl-ZrF_4, and LiCl-KCl-LiF-$ZrCl_4$ salts. The potential scan began from an open circuit potential (OCP, ~-0.9 V) and was scanned through cycles ranging from -1.1 V to -0.4 V, -1.2 V to -0.4 V, and -1.5 V to -0.4 V vs. Ag/Ag^+ at a scan rate of 50 mV s^{-1} in the respective molten salt system. Chronoamperometric and chronopotentiometric experiments were also performed to recover Zr on the cathode from Zircaloy-4 or Zirlo cladding tube anode. The surface morphologies and crystallographic textures of cathodic deposits were characterized by field emission-scanning electron microscopy (FE-SEM, Hitachi SU8010) and an X-ray diffractometer (XRD, Bruker D8 Advance, Cu Kα=1.5418 Å), respectively. For a quantitative measurement of the recovered Zr, inductively coupled plasma-atomic emission spectroscopy (ICP-AES), atomic adsorption spectroscopy (AAS), and ion chromatography (IC) were used.

3. RESULTS AND DISCUSSION

Cyclic voltammetries for Zr reduction/oxidation were performed at a scan rate of 50 mV s^{-1} in 600 ^oC LiCl-KCl-0.07 M $ZrCl_4$ salts as shown in Fig. 1a. The potential scan was repeated three times for various switching potentials. In agreement with the results for 500 ^oC LiCl-KCl-$ZrCl_4$ salts in other literatures [18,20,25], the reduction of Zr (IV) reveals to occurs through a multi-step reaction, although the two major peak positions are positively shifted from -1.15 V to -1.02 V and from -1.55 V to -1.33 V compared to the previous work that we performed at 500 ^oC [8]. The preliminary experiment showed that the peak potentials are found to be gradually shifted toward a positive direction as the operating temperature increases from 400 ^oC to 600 ^oC. Assuming that the Zr reduction/oxidation process at 600 ^oC is analogous to that at 500 ^oC, the following reactions are expected to be overlapped at respective peak potential.

$$Zr^{4+} + 3e^- \rightarrow Zr^+$$
$$Zr^{2+} + 2e^- \rightarrow Zr \qquad E_p = -1.02 \text{ V} \qquad (1)$$

$Zr^{+} + e^{-} \rightarrow Zr$
$Zr^{4+} + 4e^{-} \rightarrow Zr$ E_p= -1.33 V (2)

However, the reaction mechanism can possibly be changed owing to the predominance of reaction depending on the operating temperature as Baboian *et al* examined [26]. In addition, a significant cathodic background current is revealed to be begun from the first cathodic peak near -1.0 V at scan rate of 50 mV s^{-1}. This might be associated with a continuous adsorption and reduction process of Zr(II) ions formed by the disproportionation reaction ($Zr(IV) + Zr \rightarrow 2Zr^{2+}$) at the electrode surface as well as an unstable complex formation between Zr^{4+} and Cl^{-} that leads to a homogenous reduction to Zr^{+}.

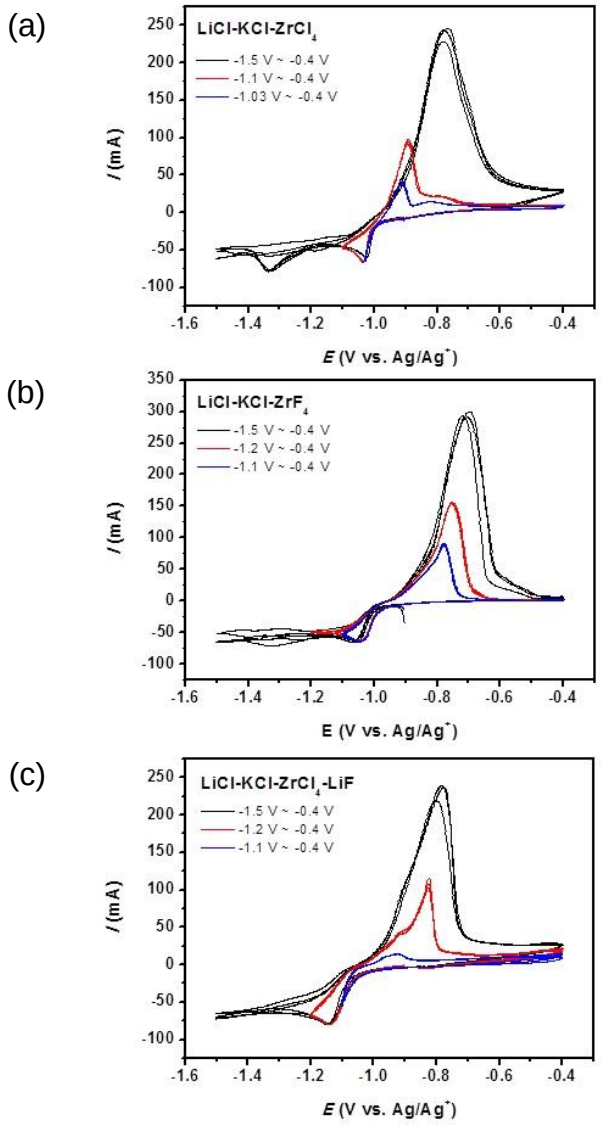

Figure 1. Cyclic voltammetric curves for Zr reduction/oxidation in various molten salts at 600 ^{o}C. (a) LiCl-KCl-0.07 M $ZrCl_4$, (b) LiCl-KCl-0.07 M ZrF_4, and (c) LiCl-KCl-0.07 M $ZrCl_4$-0.84 M LiF. A tungsten wire and Zr rod were used as working and counter electrodes, respectively. The potential of the working electrode was scanned three times at 50 mV s^{-1} in various ranges for each electrolyte.

When fluoride ions were added as a form of initiator such as ZrF_4, a decrease in the reduction peak at -1.33 V is revealed with a subtle shift of the peak at -1.02 V toward the negative direction as shown in Fig. 1b. However, no ultimate change is seen in the reduction behavior of Zr compared to that of the all-chloride bath. This reflects that Zr cations are not fully complexed with fluoride ions because the molar ratio of F^-/Zr^{4+} is fixed as 4, while the Zr(IV) complexes are known to have coordination numbers of 6 (eg., $[ZrCl_6]^{2-}$ or $[ZrF_6]^{2-}$). Therefore, mixed fluoro-chloro Zr complexes might be involved with the following reduction processes, when the molar ratio of F^-/Zr^{4+} is less than 6, depending on the concentration of fluoride ions [22].

$$ZrCl_{6-x}F_x^{2-} + e^- \rightarrow ZrCl_{6-x}F_x^{3-} \quad [3]$$

$$ZrCl_{6-x}F_x^{3-} + 3e^- \rightarrow Zr + (6-x)Cl^- + xF^- \quad [4]$$

However, when the molar ratio of F^-/Zr^{4+} was controlled at above 6 by changing the concentration of F^- with LiF in LiCl-KCl-$ZrCl_4$ salts, the reduction behavior of Zr was revealed to be significantly changed, as shown in Fig. 1c. Only a single reduction peak at -1.15 V is evident, which is assumed to be associated with the following one-step reduction process.

$$[ZrF_6]^{2-} + 4e^- \rightarrow Zr + 6F^- \quad [5]$$

This indicates direct evidence that Zr complexes in molten salts can be modified by changing the anions. According to the free energies of formation of metal halides in the gas phase [27], the order of affinity for halide ions with Zr^{4+} cations is $F^- > Cl^- > Br^- > I^-$, which means Zr-fluoride complexes are more stable compared to Zr-chloride complexes. The difference in the reduction mechanism can be analogized from the oxidation peaks at various scan ranges. For the full scan range of -0.4 V to -1.5 V, the oxidation peaks for Zr to Zr(IV) appears to be similar between the LiCl-KCl-$ZrCl_4$ and LiCl-KCl-$ZrCl_4$-LiF salts. However, when the potential scan was limited to -1.1 V for LiCl-KCl-$ZrCl_4$ salt, the oxidation peak corresponding to the first reduction peak at -1.02 V appears to be at -0.9 V, which might be associated with the following oxidation reactions.

$$Zr^+ \rightarrow Zr^{4+} + 3e^- \quad [6]$$

$$Zr \rightarrow Zr^{2+} + 2e^- \quad [7]$$

The superposed shoulder peak at about -0.91 V might be associated with the oxidation reaction of pre-existing Zr^{2+} ions by disproportionation reaction to Zr^{4+}.

On the other hand, in the case of LiCl-KCl-$ZrCl_4$-LiF salts, the cathodic potential scan down to -1.2 V, which is the vicinity of the single reduction peak, leads the oxidation peak to be prominent at a more positive potential, ~ -0.84 V, which might be attributed to the following reaction.

$$Zr \rightarrow Zr^{4+} + 4e^- \quad [8]$$

Even for the LiCl-KCl salts added with ZrF_4, the oxidation peak corresponding to the reduction at -1.05 V is revealed to be shifted toward the positive direction compared to the all-chloride salts, which might be caused by the oxidation of metallic Zr reduced from Zr ions that are partially complexed with fluoride ions in the potential regime examined.

Based on the results of the voltammetric scans, electrorefining experiments were performed on W wire cathodes with Zircaloy-4 and Zirlo tubes as anodes by applying a constant current or potential in various molten salt systems.

Figure 2 shows photo images of Zr deposits electrorefined at -1.1 V vs. Ag/Ag^+ in 600 ^oC LiCl-KCl-$ZrCl_4$ and LiCl-KCl-ZrF_4 molten salts. As found in the difference of the oxidation behavior of Zr

that is reduced on the cathode, the morphological feature of the Zr deposit is distinguished between LiCl-KCl-$ZrCl_4$ and LiCl-KCl-ZrF_4, as shown in Fig. 2. A dendrite-like Zr deposit is revealed for the chloride-based molten salts added with ZrF_4 as the initiator, while the powdery Zr is evident with residual salts intercalated between the deposits for LiCl-KCl-$ZrCl_4$ salts.

Figure 2. Photo images of Zr deposits electrorefined in (a) LiCl-KCl-0.07 M $ZrCl_4$ and (b) LiCl-KCl-0.07 M ZrF_4. The applied potential was -1.1 V vs. Ag/Ag^+.

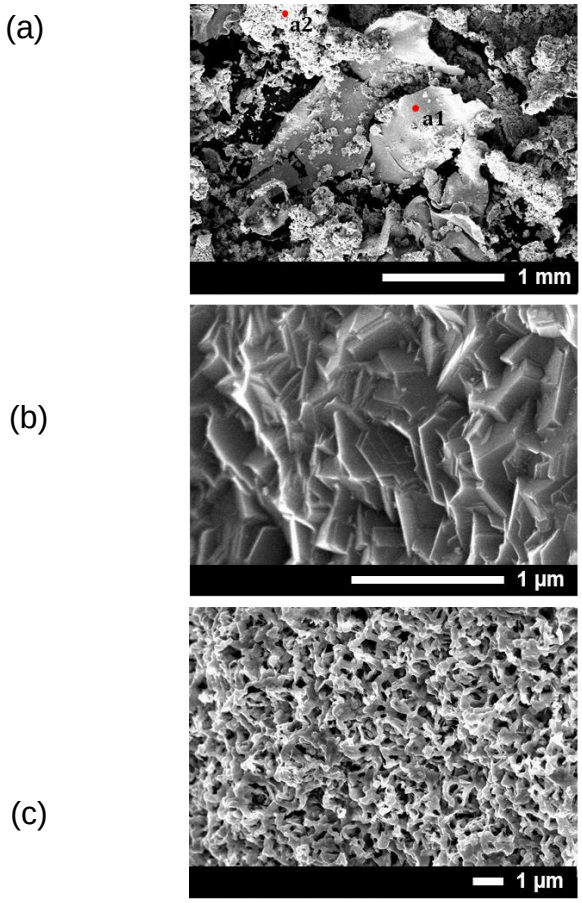

Figure 3. SEM images of cathodic Zr deposits electrorefined at 600 ^oC in LiCl-KCl-ZrF_4 molten salts. (a) Low magnification (x40), (b) position a1, and (c) position a2.

After the chronoamperometric experiments at a constant potential, a color difference was found between the all-chloride and fluoro-chloro mixed salts. The solidified LiCl-KCl-$ZrCl_4$ salt revealed to be dark yellow in color, which results from the formation of Zr(II) by the disproportionation reaction. On the other hand, fluoride-added LiCl-KCl salts were close to white in color after the experiment, which is indirect evidence that the presence of fluoride ions stabilizes the higher oxidation states of Zr. The stabilization of Zr(IV) ions is believed to be one of factors that improved the quality of Zr deposit [28].

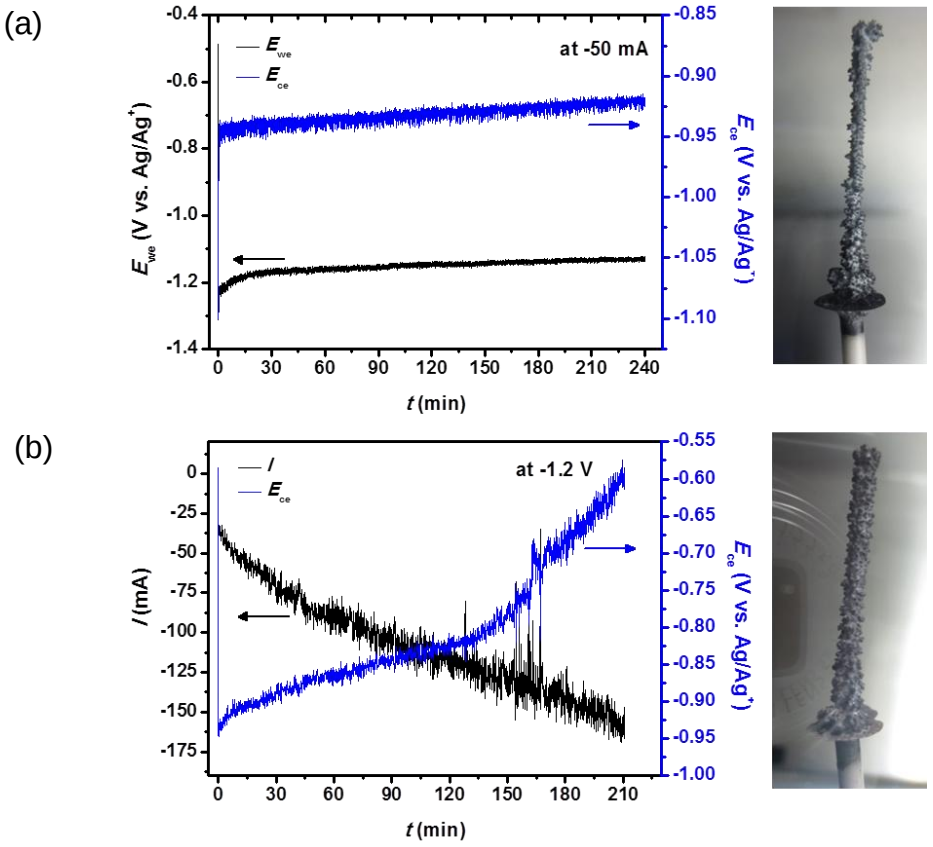

Figure 4. (a) Chronopotentiometric and (b) chronoamperometric curves for Zr electrorefining of Zirlo cladding tubes (left) in 600 ^oC LiCl-KCl-$ZrCl_4$-LiF molten salts and photo images of the cathodic products for the respective process (right). The applied current and potential were maintained at -50 mA for 4 h and at -1.2 V (vs. Ag/Ag^+) for 3.5 h, respectively. The E_{we} and E_{ce} represent the potentials for working and counter electrode, respectively.

The microstructure of the cathodic deposit electrorefined in LiCl-KCl-ZrF_4 salts was observed by FE-SEM, as shown in Fig. 3. A low magnification of the deposit prepared by salt dissolution in a diluted hydrochloric acid followed by drying in an aspirator reveals that metallic plates (a1) are mixed with a dark powdery substance agglomerated with each other (a2). As shown in the magnified image for position a1 in Fig. 3b, metallic crystal facets are evident, which were identified as Zr metal over 99 wt% by an EDX analysis. Despite the different surface morphology, the Zr content for position a2 was

revealed to be more than 96 wt% with about 2 wt% O and 1 wt% F. This is considered to be caused by a partial dissolution of Zr subchlorides that are soluble through a hydrolysis reaction in water or diluted hydrochloric acid [29].

The electrorefining experiments for Zirlo tubes in LiCl-KCl-LiF-$ZrCl_4$ were performed on W wire cathodes at a constant potential and current, as shown in Fig. 4. Chronopotentiometric curve at -50 mA exhibits almost a constant potential that starts from about -1.2 V and converges to about -1.15 V for 240 min. The anodic potential also appears to be stable at -0.925 V. On the other hand, chronoamperometric curve at -1.2 V shows a gradual increase in the cathodic current transient toward the negative direction with significant noise. This might be associated with an expansion of the electrode surface and a gradual decrease in the distance between the cathode and anode according to the growth of Zr. However, the morphological features of the Zr deposit electrorefined by two different techniques appear to be similar as a dendritic form, although the amount of deposit was different due to a difference in the total current flown.

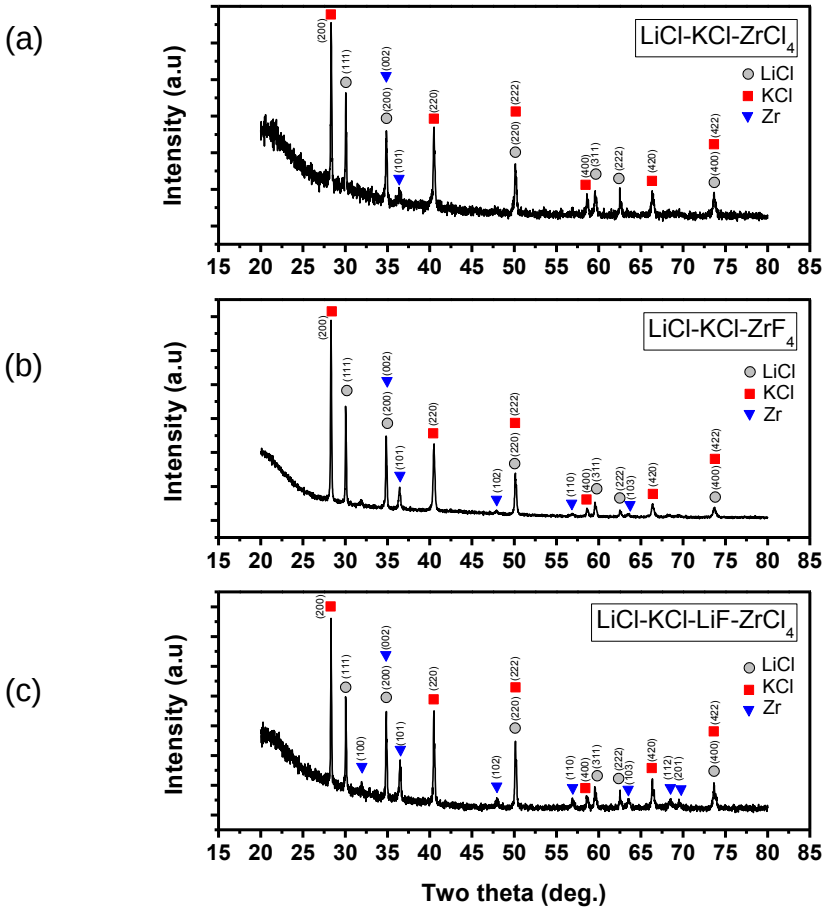

Figure 5. X-ray diffraction patterns of the recovered Zr deposits at 600 ^{o}C in various molten salts. (a) -1.0 V (vs. Ag/Ag^{+}) for 3 h in LiCl-KCl-$ZrCl_4$, (b) -1.1 V (vs. Ag/Ag^{+}) for 2 h and 30 min in LiCl-KCl-ZrF_4, and (c) -1.1 V (vs. Ag/Ag^{+}) for 3 h in LiCl-KCl-LiF-$ZrCl_4$.

X-ray diffraction (XRD) patterns for the electrorefined Zr from various molten salt systems are shown in Fig. 5. The samples were prepared by finely grinding the recovered Zr containing residual salts in the glove box and transferred into air-tight holders for XRD measurements. A high background at low angles is attributed to a dome-like X-ray transparent cap of the airtight holder. The XRD peaks corresponding to LiCl and KCl are evident for all samples due to the solidified salt in the deposit during the cooling process. Although the Zr (002) peak at 34.8^o is overlapped with the LiCl peak, the relative intensities of metallic Zr peaks with different textures become stronger in comparison with those of salt peaks in the order of LiCl-KCl-LiF-$ZrCl_4$ > LiCl-KCl-ZrF_4 > LiCl-KCl-$ZrCl_4$, which is an indication of the morphology improvement, which leads to the prevention of salt incorporation. In addition, the FWHM (full-width at half maximum) value of Zr (101), a preferred orientation for Zr hcp, was slightly decreased from 0.27^o in LiCl-KCl-ZrF_4 salts to 0.24^o in LiCl-KCl-LiF-$ZrCl_4$ salts, which implies an increase in the crystallite size by the Debye-Scherrer relationship.

Table I. Quantitative measurement of Zr deposits electrorefined in two different molten salt systems using ICP-AES for Zr, Sn, and Fe, AAS for Li and K, and IC for Cl^- and F^-. The electrorefining potential was applied at -1.1 V vs. Ag/Ag^+ for 2 h and 30 min in LiCl-KCl-ZrF_4 and for 3 h in LiCl-KCl-LiF-$ZrCl_4$ salts.

Components (wt%)	Type of molten salt	
	LiCl-KCl-ZrF_4	LiCl-KCl-LiF-$ZrCl_4$
Zr	18.29	38.99
Sn	0.005	0.135
Fe	0.005	0.008
Li	6.74	11.61
K	24.17	14.44
Cl^-	50.41	34.46
F^-	0.15	0.478
etc.	0.27	0.005

Table I shows the results of quantitative measurements for Zr deposits electrorefined from LiCl-KCl-ZrF_4 and LiCl-KCl-LiF-$ZrCl_4$ salts, respectively. The samples were identically prepared as XRD measurement. It was assumed that the residual salt adhered to the surface flew down because the electrode assembly was hold in a heating zone of the reactor for 1 hr after lifting it up from the electrolyte. The deposit of 0.3 g from each salt was sampled for ICP-AES, AAS, and IC measurements. In previous work, the Zr content in the cathodic deposit was limited to about 5 wt% for

LiCl-KCl-$ZrCl_4$ owing to the salt incorporation, even though the Zr purity was high enough to be above 99 wt% [9]. However, the addition of fluoride compounds increased the Zr content up to 18.29 wt% for LiCl-KCl-ZrF_4 and up to 38.91 wt% for LiCl-KCl-LiF-$ZrCl_4$ salts, as shown in Table I. On the other hand, salt contents such as K, Cl^- were decreased from 24.17 wt% and 50.41 wt% to 14.44 wt% and 34.46 wt%, respectively. The concentrations of Li and F^- slightly increased because of the addition of LiF.

4. CONCLUSIONS

The effect of adding fluoride compounds in the Zr electrorefining of Zirlo cladding tubes was examined using cyclic voltammetries. The multi-step reduction process of Zr, evident at -1.02 V and -1.33 V vs. Ag/Ag^+ in 600 ^oC LiCl-KCl-0.07 M $ZrCl_4$ salts, was slightly changed with a noticeable shift in the oxidation peak position by the replacement of the initiator with the same molar concentration of ZrF_4. However, a more remarkable change was evident in the voltammetric behavior of Zr to a single-step reduction at -1.15 V vs. Ag/Ag^+, when the molar ratio of F^-/Zr^{4+} was independently controlled to be over 6 by the addition of 0.84 M LiF in 600 ^oC LiCl-KCl-0.07 M $ZrCl_4$ salts.

The morphological features of Zr deposits electrorefined from Zirlo tubes were also changed from a powder-type to dendritic crystals in the chloride-fluoride mixture molten salts, which led to a reduction of the salt incorporation. The crystallinity of metallic Zr was also enhanced by the addition of fluoride ions. Chloride-based salts mixed with fluoride ions are expected to be more advantageous compared to all-chloride or all-fluoride baths in terms of the process applicability for the treatment of cladding hull wastes.

ACKNOWLEDGEMENT
This work was supported by the National Research Foundation of Korea (NRF) grant funded by the Korean Ministry of Science, ICT and Future Planning (No. 2012M2A8A5025699).

References

1. J. P. Ackerman, *Ind. Eng. Chem. Res.*, 30 (1991) 141.
2. J. J. Laidler, J. E. Battles, W. E. Miller, J. P. Ackerman and E. L. Carls, *Prog. Nucl. Energ.*, 31 (1997) 131.
3. H. Lee, J.-M. Hur, J.-G.Kim, D.-H.Ahn and Y.-Z. Cho, *Energ. Procedia*, 7 (2011) 391.
4. T. S. Rudisill, *J. Nucl. Mater.*, 385 (2009) 193.
5. U.S. Japan Joint Nuclear Energy Action Plan Waste Management Working Group Phase I Report, U. S. Department of Energy, FCR&D-USED-2010-000051 (2010).
6. International Atomic Energy Agency, Technical Reports Series No. 258, IAEA Vienna (1985).
7. R. Fujita, H. Nakamura, K. Mizuguchi, M. Sato, T. Shibano, Y. Ito, T. Goto, T. Terai and S. Ogawa, *Electrochem.*, 73 (2005) 751.
8. C. H. Lee, K. H. Kang, M. K. Jeon, C. M. Heo and Y. L. Lee, *J. Electrochem. Soc.*, 159 (2012) D463.

9. C. H. Lee, M. K. Jeon, C. M. Heo, Y. L. Lee, K. H. Kang and G. I. Park, *J. Electrochem. Soc.*, 159 (2012) E171.
10. C. H. Lee, Y. L. Lee, M. K. Jeon, Y. T. Choi, K. H. Kang and G. I. Park, *J. Nucl. Mater.*, 449 (2014) 93.
11. Chintamani, N. Saratchandran, P. Pande, A. K. Taneja and J. C. Sehra, in *Zirconium in the Nuclear Industry: Seventh International Symposium*, Adamson and V. Swam, Editors, p. 136, ASTM Publication, Philadelphia (1987).
12. B. Gilbert, G. Mamantov and K. W. Fung, *Inorganic Chem.*, 14 (1975) 1802.
13. F. Basile, E. Chassaing and G. Lorthioir, *J. Appl. Electrochem.*, 11, 645 (1981).
14. L. P. Polyakova and P. T. Stangrit, *Electrochim. Acta*, 11 (1982) 1641.
15. G. J. Kipouros and S. N. Flengas, *J. Electrochem. Soc.*, 132 (1985) 1087.
16. C. Guang-Sen, M. Okido and T. Oki, *J. Appl. Electrochem.*, 20 (1990) 77.
17. M. Yamane and R. Takagi, *Denki Kagaku*, 60 (1992) 900.
18. Y. Sakamura, *J. Electrochem. Soc.*, 151 (2004) C187.
19. H. Groult, A. Barhoun, H. El Ghallali, S. Borensztjan and F. Lantelme, *J. Electrochem. Soc.*, 155 (2008) E19.
20. S. Ghosh, S. Vandarkuzhali, P. Venkatesh, G. Seenivasan, T. Subramanian, B. P. Reddy and K. Nagarajan, *J. Electroanal. Chem.*, 627 (2009) 15.
21. G. M. Martinez and D. E. Couch, *Metall. Trans.*, 3 (1972) 571.
22. A. Girginov, T. Z. Tzvetkoff and M. Bojinov, *J. Appl. Electrochem.*, 25 (1995) 993.
23. J. A. Gurklis, J. G. Beach and C. L. Faust, Report No. BMI-781, Battelle Memorial Institute, Columbus, Ohio (1952).
24. G. W. Mellor and S. Senderoff, *J. Electrochem. Soc.*, 113 (1966) 60.
25. J. Park, S. Choi, S. Sohn, K. R. Kim and I. S. Hwang, *J. Electrochem. Soc.*, 161 (2014) H97.
26. R. Baboian, D. L. Hill and R. A. Bailey, *J. Electrochem. Soc.*, 112 (1965) 1221.
27. A. E. Martell and R. D. Hancock, *Metal Complexes in Aqueous Solutions* in Modern Inorganic Chemistry Series, 15, Plenum Press, New York and London (1996).
28. F. Lantelme and A. Salmi, *J. Electrochem. Soc.*, 142 (1995) 3451.
29. F. Basile, E. Chassaing and G. Lorthioir, *J. Less-Common Met.*, 98 (1984) 1.